

## PHOTOGRAMMETRIC MEASUREMENT OF LINEAR OBJECTS WITH CCD CAMERAS – SUPER-ELASTIC WIRES IN ORTHODONTICS AS AN EXAMPLE

Tim SUTHAU<sup>1)</sup>, Matthias HEMMLEB<sup>1)</sup>, Dietmar ZURAN<sup>2)</sup>, Paul-Georg JOST-BRINKMANN<sup>2)</sup>

<sup>1)</sup>Technical University of Berlin, Germany  
Department for Photogrammetry and Cartography  
tim@fpk.tu-berlin.de

<sup>2)</sup>Charité, Medical Faculty of the Humboldt University of Berlin, Germany  
School of Dentistry, Department of Orthodontics and Dentofacial Orthopedics  
dietmar.zuran@charite.de

Working Group V/1

**KEY WORDS:** Calibration, CCD, Medicine, Object recognition, Orthodontics, Photogrammetry, Recognition

### ABSTRACT

This paper describes the development of an approach for nearly automatic recognition of the shape of linear objects on the example of super-elastic wires in orthodontics. This is made possible by the integration of known parameters which describe the general shape of the objects concerned. Such parameters are derived from the production process of these objects. A digital photogrammetric 3D measurement system should give a touchless measurement of the wires. The images were taken with two CCD cameras.

The goal was to find specific algorithms for object recognition and to apply them to the measurement of the wires. The algorithm should guarantee an automatic extraction of edges of a linear object by model based procedures in the image. In this case, a 3D model should be derived from the parameters controlling the production process. It should be introduced into the algorithm as a base of knowledge. As a result we get new 3D coordinates of the vertices of the wires. The edge lengths and the bending and torsion angles between the vertices could be derived from these coordinates. Afterwards the results were compared with the parameters of the bending machine, and the accuracy of the photogrammetric procedure was evaluated.

### 1 INTRODUCTION

For many years photogrammetric procedures have significantly contributed to the touchless measurement of objects of all kind. Especially the introduction of digital image processing techniques has opened new fields of applications for photogrammetry. Digital image processing is an efficient tool to derive geometrical information from digital imagery in a fast and economic way. In recent years versified approaches for object recognition as well as ways for extraction of geometrical information were developed for very different applications.

This paper describes the development of an approach for nearly automatic recognition of the shape of linear objects. This is made possible by the integration of known parameters which describe the general shape of the objects concerned. Such parameters are derived from the production process of these objects. The procedure was tested by applying it to the measurement of angulations in super-elastic wires. These memory-NiTi-wires to be examined are used during orthodontic treatments. A bending system which controls a bending machine via a CNC batch file is used for shaping the wires. The memory-form is programmed into the wires by a special heat treatment, so that, at a specific temperature, the wires somewhat return into their initial configuration. The used procedure ought to check the setting values at the bending machine. A digital photogrammetric 3D measurement system was applied for image acquisition. The images were taken with two CCD cameras which were connected to a workstation via a video board. Program modules for the photogrammetric restitution, e.g. for calibration and for point determination, were available.

The goal was to find specific algorithms for object recognition and to apply them to the measurement of the wires. The algorithm should guarantee an automatic extraction of edges of a linear object by model based procedures in the image. In this case, a 3D model has to be derived from the parameters controlling the production process. It should be introduced into the algorithm as a base of knowledge. As a result new 3D coordinates of the vertices of the wires are obtained. The edge lengths and the bending and torsion angles between the vertices can be derived from these coordinates. Afterwards the results were compared to the parameters of the bending machine.

From investigations on the accuracy of the procedure it is possible to evaluate the applicability of the approach. One has to distinguish between the accuracy of the calibration of the cameras, the accuracy of the algorithm for the location of the edges and vertices, and the absolute accuracy of the overall system. The assignment is to verify the angles, accordingly the relative accuracy is to be examined. Furthermore, the applicability of this procedure to similar tasks must be considered. In general, linear objects of every kind (e.g. wires of every size, pipes, etc.) or objects with linear edges (concrete slabs) can be treated if model data (e.g. in the form of a CAD) are available.

## 2 IMAGE DATA ACQUISITION AND THE CONFIGURATION OF THE SYSTEM

### 2.1 Image data acquisition

In this work, two commonly available CCD cameras of the type SONY XC 77CE were employed, which were connected over a frame grabber. The technical data of the cameras are listed in Table 1.

Type of the camera	SONY XC 77CE
Number of pixels	756 columns, 581 rows
Signal transfer	Analogue composite video-signal (CCIR)
Pixel size	11,0 x 11,0 $\mu\text{m}$
Lens	focal length 16 mm

Table 1. Technical data of the camera

A CCD camera can be understood as a metric camera because of its solid CCD matrix. It is assumed that the lens is stably interconnected with the camera body and the focal length is fixed. The interior orientation of the cameras must either be available or has to be calculated together with the exterior orientation during the calibration of the cameras.

### 2.2 Configuration of the system

The configuration of the measurement corresponds to the case of aerophotogrammetry (Figure 1). The definition of the rotation that is necessary to describe the position of the cameras, is shown in Figure 1. For the determination of an appropriate configuration and the calculation of the camera parameters the following input was used:

- object size,
- principal distance and
- the size of the digital image.

The distance between object and camera was fixed on 30 cm, because the focal length is on the nearest position (stop-position). With this configuration the photogrammetric restitution of objects with a size of approximately 12·16 cm<sup>2</sup> is possible. The depth of focus amounts 15 cm.

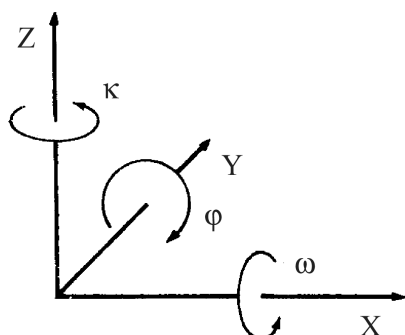


Figure 1. Definition of rotation

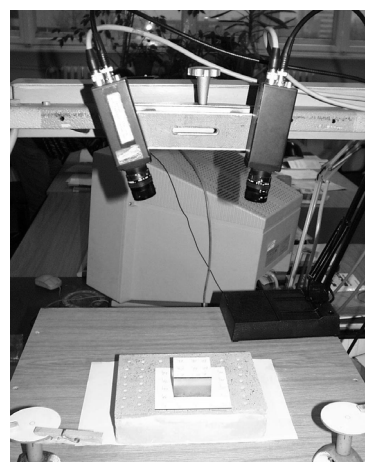


Figure 2: Camera configuration

### 3 PHOTGRAMMETRIC PROCESSING

#### 3.1 Calibration

Due to the configuration of the system (Figure 2), the calibration object consists of a base-plate (10·10 cm<sup>2</sup>) with 16 control points and an attached cube (5·5·3 cm<sup>3</sup>) with 9 control points (Figure 3)

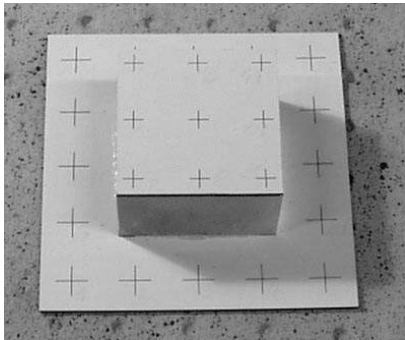


Figure 3: Calibration object

A bundle adjustment was applied for calibration of the CCD camera. Thus we determine the parameters of the interior orientation of the cameras and the calibration of the whole system (including the exterior orientation) in one step. For the central perspective condition, the following equations were employed:

$$x' = x'_H - c_k \cdot \frac{d_1 \cdot (X - X_0) + d_2 \cdot (Y - Y_0) + d_3 \cdot (Z - Z_0)}{d_7 \cdot (X - X_0) + d_8 \cdot (Y - Y_0) + d_9 \cdot (Z - Z_0)} \quad (1)$$

$$y' = y'_H - c_k \cdot \frac{d_4 \cdot (X - X_0) + d_5 \cdot (Y - Y_0) + d_6 \cdot (Z - Z_0)}{d_7 \cdot (X - X_0) + d_8 \cdot (Y - Y_0) + d_9 \cdot (Z - Z_0)} \quad (2)$$

For the distortion model, the following equations were employed:

$$x' = \Delta x' + x' \quad (3)$$

$$y' = \Delta y' + y' \quad (4)$$

$$\Delta x' = k_1 \cdot (x'^3 + x' \cdot y'^2) \quad (5)$$

$$\Delta y' = k_2 \cdot (y'^3 + x'^2 \cdot y') \quad (6)$$

with

- $x', y'$  - image coordinates
- $X, Y, Z$  - coordinates of object points
- $d_i$  - rotation matrix
- $c_k, x'_h, y'_h, \Delta x', \Delta y'$  - interior orientation (for each camera)
- $X_0, Y_0, Z_0, \Phi, \Omega, \kappa$  - exterior orientation (for each image)
- $k_1, k_2$  - parameters for radial lens distortion

In the experiment, the calibration object was taken at a distance of approximately 30 cm and at the principal distance of 15,30 mm from the CCD camera from 9 different directions and positions, in such a way that the images could be overlapped 100%. In order to test the absolute accuracy of the configuration, we calculated the bundle adjustment with determination of the calibration points as new points. The achieved accuracy of the 3D measurement is 0,1 mm in X- and Y-direction and 0,4 mm in Z. In order to attain a better accuracy it would be necessary to enhance the distortion parameters and to use a calibration object with more accurate calibration points.

### 3.2 Photogrammetric processing model

The photogrammetric calibration delivers the orientation parameters of the cameras and the whole system. With the application of these parameters and the measurements in the images of the represented object it is possible to derive 3D coordinates of this object. The measurement of image coordinates took place with methods of digital image processing. It was a combination between different image processing operations, like edge extraction and vectorisation. A system overview is illustrated in Figure 4.

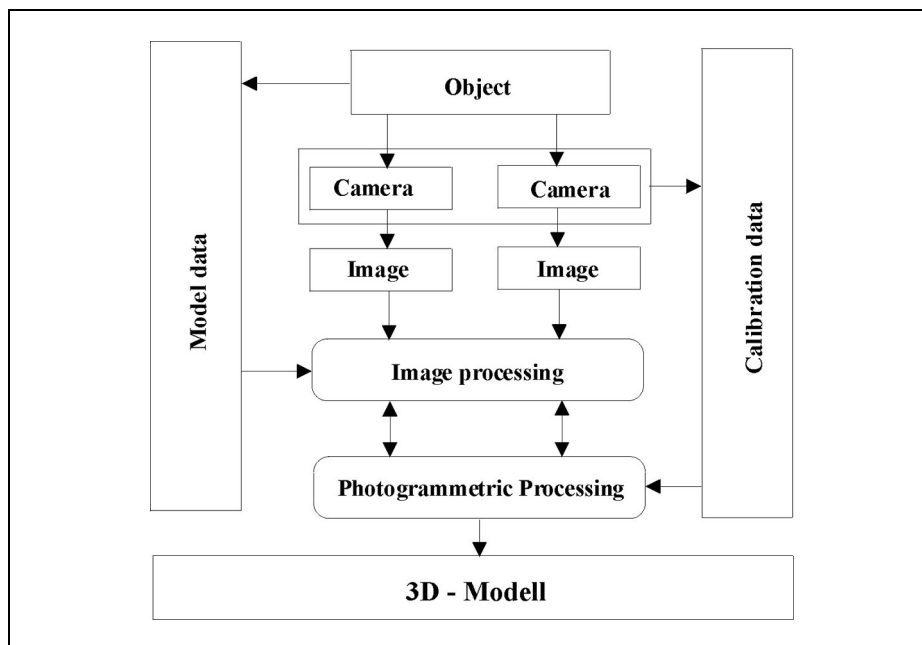


Figure 4. System overview

### 3.3 Evaluation of the object

The task was to survey super elastic wires. As mentioned above, these memory-NiTi-wires to be examined are used during orthodontic treatments. A bending system which controls a bending machine via CNC batch file is used for shaping the wires. The input data for shaping the wires are the edge lengths and the bending and torsion angles between the vertices. These values should be checked. In order to achieve the comparison between the parameters of the bending machine and the actually existing values of the wire all the steps illustrated in Figure 5 were necessary.

#### 3.3.1 Providing model coordinates

In the first step a 3D model has to be derived from the parameters controlling the production process. The CNC batch file contains the edge length between the vertices (= distance  $s_{[i]}$ ), the bending angles (from it the azimuth  $t_{[i]}$ ) and the torsion angles. From these parameters the coordinates of the model were calculated:

$$\begin{aligned}
 x_{[i+1]} &= x_{[i]} + s_{[i]} \cdot \cos t_{[i]} \\
 y_{[i+1]} &= y_{[i]} + s_{[i]} \cdot \sin t_{[i]}
 \end{aligned}
 \tag{7, 8}$$

In this work only wires without torsion were examined. If it is intended to measure wires with torsions the equation has to be enhanced. In order to determine the searched vertices a backprojection of the model coordinates in the images is necessary. In accordance with the evaluation plan of the object (Figure 5), based on the information about the interconnection of points, a new enhanced edge data file was generated including azimuth and the distance of the edge.

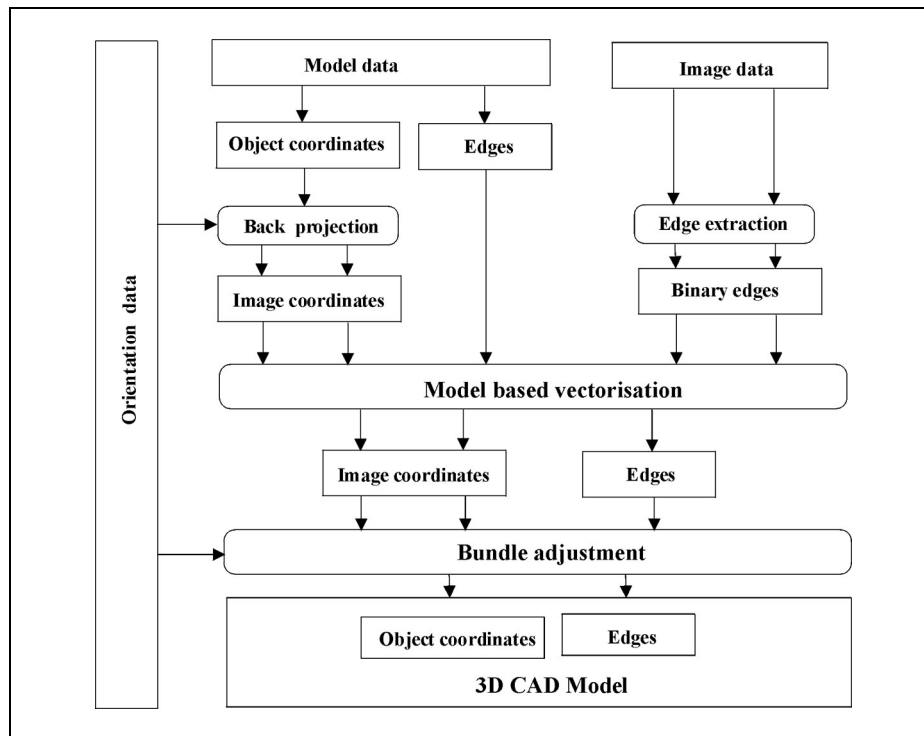


Figure 5. Flow chart for data processing

### 3.3.2 Edge extraction

Further experiments achieved reasonable results on the basis of the canny operator. The accuracy of the measured vertices and calculated angles depends on the quality of the canny operator and on the following vectorisation (chapter 3.3.3). The result of the canny operator depends on the used threshold method and on the image acquisition conditions. The ascertainment of the threshold occurred on screen. The suitable threshold is used as a definite value for all wires, which were measured under the same conditions.

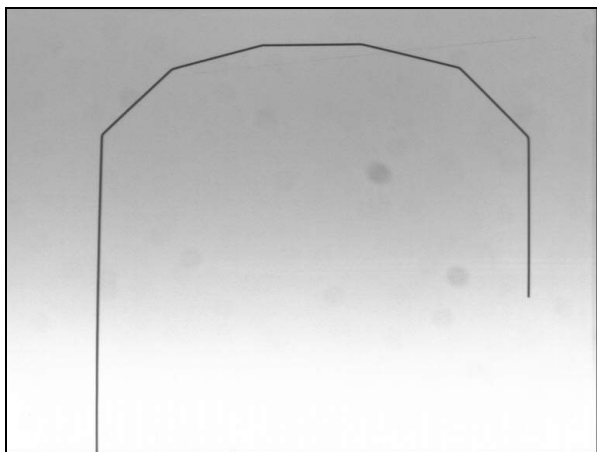


Figure 6. Original image of a wire

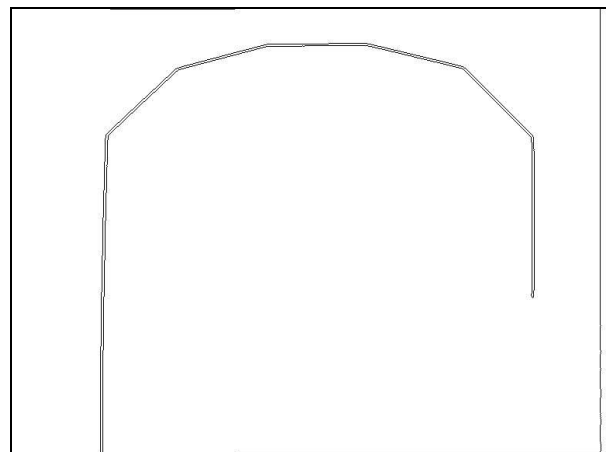


Figure 7. Edge image from Figure 6

Therefore, the prerequisite is given for an automation of the measurement. The image acquisition conditions of the wires could be optimised on the basis of the structure of the wires. We put wires on a light table and we achieved a very good contrast between the object and the surrounding area. Also shadow and shine effect, that appear with metallic workpieces otherwise, could be prevented this way. This high brightness difference is optimal for the edge extraction. The original image and the corresponding edge image are illustrated in Figure 6 and 7.

### 3.3.3 Vectorisation

An algorithm was developed for the determination of the vertices. A searching area, in which the vertices, that describe the object, are suspected, could be calculated with the help of the model data. All edges in this searching area were detected and used for the calculation of a regression straight line. The intersection of these straight lines delivers the desired coordinates of the vertices as result. This method has the advantage that edges with a certain thickness are reduced to a central axis.

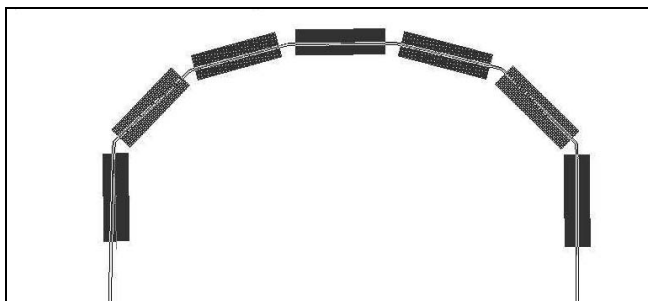


Figure 8. Searching area for the vectorisation

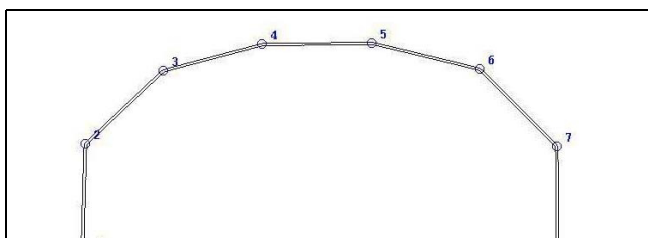


Figure 9. Edge image with the points after the vectorisation

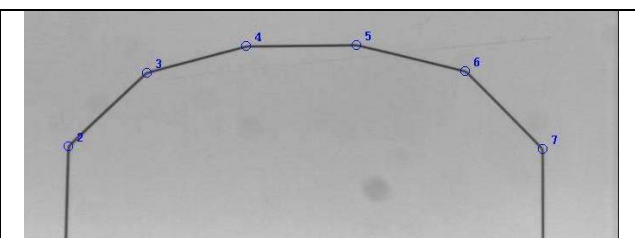


Figure 10. Original image with the points after the vectorisation

### 3.3.4 Determination of object coordinates

After the detection of vertices in the images of both cameras, these vertices could be transformed into the object area on the basis of the bundle adjustment with the help of orientation parameters. There was no problem with the assignment of homologous points because the new vertices could be named after their corresponding model points.

### 3.3.5 Derivation of distances, bending and torsion angles from object coordinates

The space distance, bending and torsion angles were calculated from the given object coordinates as follows:

#### 1) Space distance

The space distance  $s_{[i]}$  between two points  $P_{[i]}, P_{[i+1]}$ :

$$s_{[i]} = \sqrt{(x_{[i]} - x_{[i+1]})^2 + (y_{[i]} - y_{[i+1]})^2 + (z_{[i]} - z_{[i+1]})^2} \quad (9)$$

#### 2) Bending angle

The bending angle between straight lines in the 3D case is described as an angle between two vectors (represented through three points  $(P_{[i-1]}, P_{[i]}, P_{[i+1]})$ ). First, the azimuth-cosine of vectors (angle between the coordinate axis) was calculated:

Vector 1 ( $P_{[i]}, P_{[i-1]}$ ):

$$\begin{aligned}\cos \alpha_1 &= (x_{[i]} - x_{[i-1]}) / \sqrt{(x_{[i]} - x_{[i-1]})^2 + (y_{[i]} - y_{[i-1]})^2 + (z_{[i]} - z_{[i-1]})^2} \\ \cos \beta_1 &= (y_{[i]} - y_{[i-1]}) / \sqrt{(x_{[i]} - x_{[i-1]})^2 + (y_{[i]} - y_{[i-1]})^2 + (z_{[i]} - z_{[i-1]})^2} \\ \cos \gamma_1 &= (z_{[i]} - z_{[i-1]}) / \sqrt{(x_{[i]} - x_{[i-1]})^2 + (y_{[i]} - y_{[i-1]})^2 + (z_{[i]} - z_{[i-1]})^2}\end{aligned}\quad (10-12)$$

Likewise Vector 2 ( $P_{[i]}, P_{[i+1]}$ ) was calculated. The desired angle  $\delta[i]$  between the vectors is

$$\delta_{[i]} = \arccos(\cos \alpha_1 \cdot \cos \alpha_2 + \cos \beta_1 \cdot \cos \beta_2 + \cos \gamma_1 \cdot \cos \gamma_2) \quad (13)$$

### 3) Torsion angle

The torsion angle is described as an angle between two planes (represented by three points). At the wires, two points of the first plane are identical with two points of the other plane. The first plane is described by ( $P_{[i-1]}, P_{[i]}, P_{[i+1]}$ ), the second plane through ( $P_{[i]}, P_{[i+1]}, P_{[i+2]}$ ). Parameters of the first plane are

$$\begin{aligned}A_1 &= ((y_{[i]} - y_{[i-1]}) \cdot (z_{[i+1]} - z_{[i-1]}) - (z_{[i]} - z_{[i-1]}) \cdot (y_{[i+1]} - y_{[i-1]})) \\ B_1 &= ((x_{[i]} - x_{[i-1]}) \cdot (z_{[i+1]} - z_{[i-1]}) - (z_{[i]} - z_{[i-1]}) \cdot (x_{[i+1]} - x_{[i-1]})) \\ C_1 &= ((x_{[i]} - x_{[i-1]}) \cdot (y_{[i+1]} - y_{[i-1]}) - (y_{[i]} - y_{[i-1]}) \cdot (x_{[i+1]} - x_{[i-1]}))\end{aligned}\quad (14-16)$$

Likewise the second plane was calculated. Standardisation of both planes:

$$N_1 = \sqrt{A_1^2 + B_1^2 + C_1^2} \quad (17)$$

$$N_2 = \sqrt{A_2^2 + B_2^2 + C_2^2} \quad (18)$$

As result the angle between the planes:

$$\tau_{[i]} = \arccos((A_1 \cdot A_2 + B_1 \cdot B_2 + C_1 \cdot C_2) / (N_1 \cdot N_2)) \quad (19)$$

(Bronstein, 1993)

The calculation of the torsion angles is of interest for the measurement of the wires only in the respect that deviations from the plane can be proved.

## 4 EVALUATION SAMPLES

### 4.1 Practical application – measurement of super-elastic wires

After the camera was calibrated successfully and the model data were prepared, the model coordinates could be projected into the respective original image. As well, the edges were extracted in the image by the canny operator. The vectorisation of the vertices of the wires took place under aid of the projected model coordinates. The search areas of the vectorisation and the result are represented in Figures 8-10. The calculation of the object coordinates was achieved with a bundle adjustment. The results are documented in Table 2. It should be noticed that the final points, on the basis of the application of straight-cuts, could not be determined again.

point	x [mm]	y [mm]	z [mm]	mx [mm]	my [mm]	mz [mm]
2	17.202	71.752	-1.326	0.054	0.055	0.255
3	32.226	86.000	-0.593	0.050	0.062	0.259
4	50.828	90.920	-1.045	0.051	0.065	0.265
5	71.248	91.227	-1.521	0.057	0.066	0.266
6	90.867	86.442	-1.762	0.067	0.063	0.262
7	104.929	71.815	-2.627	0.076	0.056	0.259

Table 2. Values of the object coordinates

The accuracy achieved of the x as well as y coordinates is about  $\pm 0,08$  mm, the accuracy of z coordinates is about  $\pm 0,27$  mm. The new spatial distances and bending angles were calculated with the help of the object coordinates with formulas (9-19). A comparison between the values of the model and the real values is documented in Table 3.

Distance from point	Model distance [mm]	Object distance [mm]	Angle between point	Angle in model [degrees]	Angle on object [degrees]
2 to 3	20,0	20.72	2,3 and 4	30,0	28,86
3 to 4	20,0	19.25	3,4 and 5	15,0	13,94
4 to 5	20,0	20.43	4,5 and 6	15,0	14,58
5 to 6	20,0	20.20	5,6 and 7	30,0	32,46
6 to 7	20,0	20.31			

Table 3. Comparison between the results and the model data

## 4.2 Evaluation of results and accuracy

With the presented algorithm good results could be achieved concerning the edge extraction and vectorisation. The achieved accuracy of the calibration is  $\pm 0,1$  mm in plane and  $\pm 0,04$  mm in height. The accuracy of the measurement of a wire achieved about  $\pm 0,08$  mm in the x as well as in y coordinate and about  $\pm 0,27$  mm in the z coordinate. This precision depends on the length of the detected straight lines and the image acquisition conditions. This accuracy is most important for the comparison of the parameters of the bending machine and the real values. The appointed accuracy corresponds to the angle accuracy  $\pm 0,25$  degrees ( $m_{x,y} = \pm 0,08$  mm,  $s = 20$  mm) and  $\pm 0,86$  degrees ( $m_z = \pm 0,27$  mm,  $s = 20$  mm). The inner accuracy was tested by a comparison between the represented algorithm and a software for automatic measurement of image coordinates. The achieved accuracy of the whole system is estimated  $\pm 0,2$  mm in plane and  $\pm 0,5$  mm in height. An expansion of the bundle adjustment using further distortion parameters and a better determined calibration object would improve the accuracy.

## 5 CONCLUSIONS

In the presented paper, an approach for nearly automatic recognition of the shape of super-elastic wires has been introduced. For industrial use, the separate program components have to be summarised and optimised. An improvement of the calibration (e.g. the extension of the distortion parameters) would lead to an increasing precision. A surveying of other objects is possible, if the pre-condition (boundary of the object through straight-pieces and existence of model coordinates) is fulfilled. The size of the object plays no role with it, but must be considered regarding the resolution and the accuracy however. Also a transfer of the system on other objects is possible. An adaptation of the vectorising algorithm would be necessary. With the presented paper it could be shown that the utilisation of CCD cameras and suitable software enables an effective surveying of objects in the field of close-range photogrammetry.

## ACKNOWLEDGEMENTS

The authors like to thank Volker Rodehorst (TU Berlin) for his implementation of the Canny operator and his suggestions in the field of image processing.

## REFERENCES

- Bronstein, I. N., Semendjajew, K. A., Musiol, G., Mühlig, H., 1993. Taschenbuch der Mathematik. 1.Auflage, Verlag Harri Deutsch, Thun, Frankfurt am Main.
- Drescher, D., Bourauel, Ch., Thier, M., 1980. Materialtechnische Besonderheiten orthodontischer Nickel-Titan-Drähte. Fortschritt Kieferorthopädie 6 (51), pp. 320-326.
- Marr, D., 1982. Vision – A Computational Investigation into the Human Representation and Processing of Visual Information. W.H. Freeman & Co., San Francisco.
- Rodehorst, V. 1997. Architectural Image Segmentation Using Digital Watersheds. In: Proc. Of the 7<sup>th</sup> Int. Conf. For Computer Analysis of Images and Patterns CAIP'97, Lecture Notes in Computer Science 1296, Editors: Sommer, G., Daniilidis, K., Pauli, J. Kiel, pp. 408-415.
- Vieweg, A., Carlsohn, M.F., 1990. Modellgesteuerte Konturverfolgung zur vollständigen Segmentierung von Bildern. Mustererkennung 1990, Springer Verlag Berlin Heidelberg.